Proceedings of the 6th International Symposium
on
Advanced Nuclear Energy Research
—INNOVATIVE LASER TECHNOLOGIES IN NUCLEAR ENERGY—

Diagnosis of Laser Ablated Carbon Particles Measured by Time-Resolved X-ray Absorption Spectroscopy

A.Miyashita, T.Ohyanagi†, O.Yoda and K.Murakami†

Department of Materials Development
Takasaki Research Establishment, JAERI
Takasaki, Gunma 370-12, Japan

†Institute of Materials Science
University of Tsukuba
Tsukuba, Ibaraki 305, Japan

The time and space resolved properties of laser ablated carbon particles were measured by X-ray absorption spectroscopy using LPX as an X-ray source. The energy density of the irradiation laser on the sample was in the range of 0.5~20J/cm^2 and the time delay was varied between 0 and 120ns. The absorption spectra exhibited several peaks originated from level to level transitions and an intense broad absorption in the energy range of C-K edge. At a delay time of 120ns, the absorption peak from 1s→2p transition of neutral carbon atom(C^0), C^-, C^+ and C^{2+} ions were observed. The absorption peak from C^0 was stronger as the probing position was closer to the sample surface and decreased rapidly with distance from the sample surface. The absorption peak C^{2+} ion was observed only at comparatively distant positions from surface. The maximum speeds of highly charged ions were faster than that of neutral atoms and negative charged ions. The neutral atom and lower charged ions were emitted from the sample even after laser irradiation. The spatial distributions of the laser ablated carbon particles in the localized helium gas environment were measured. In the helium gas environment, the ablation plume was depressed by the helium cloud generated on the top of ablation plume.

keywords: Laser ablation, Carbon cluster, XAFS, Time-resolved measurement

1. INTRODUCTION

Laser produced plasma X-rays (LPX) have many interesting properties when used as a source of soft X-ray absorption spectroscopy. (1) The energy range of produced X-rays is from 100eV to a few keV, which covers K-absorption edges of low-Z elements such as carbon, nitrogen, oxygen, aluminum and silicon, and L-absorption edges of medium-Z elements. (2) The X-ray intensity per pulse is high enough to perform the single shot measurement[1]. (3) The X-ray pulse width is as short as the incident laser pulse width[2]. (4) The X-ray energy distribution depends on the electronic structure of the target material, which makes it easy to get both line and continuum radiations by choosing an appropriate

target. Therefore, LPX is a quite an attractive X-ray source for the dynamic investigations of materials composed of light elements[3].

Recently, laser ablation is recognized to be well suited for formation of new materials such as carbon cluster[4-5] and high T_c superconducting thin films[6]. Properties of carbon cluster, especially carbon fullerene (C_{60}, etc.), are very hot topics in the physical and chemical field. It is important to understand how they are formed in clusters or crystals. However, behaviors of the laser ablated species are not clear yet.

We have developed a time-resolved X-ray absorption spectroscopy apparatus using LPX. In this paper, we report the time evolution of the electronic structures of laser ablated carbon particles and their spatial distributions using this spectrometer. The wavelength of the irradiation laser was 532nm (Nd:YAG-SHG), the energy density on the carbon sample was in the range of 0.5~20 J/cm^2 and the time delay between sample irradiation and probe X-ray pulse was varied up to 120 ns.

2. CONSTITUTION OF THE APPARATUS

Figure 1(a) shows a schematic diagram of our spectrometer. The apparatus is composed mainly of two parts: the laser system and the spectrometer. A 20J Q-switched Nd:YAG/glass laser is used both to produce soft X-rays and to irradiate samples. The FWHM of the laser pulse is about 12ns. The fundamental laser pulse of 1064nm is frequency-doubled with the use of second harmonics generators (SHGs). The first SHG(SHG_1) generate 7J, 532nm beam. The 7J beam is focused on the cylindrical target, 40mm in diameter and 25mm long, with condenser lens (L_1). The focus size on the target is about 100μm in diameter, in this case, target irradiance power density reaches 7×10^{12}W/cm^2, and hot and dense laser plasma generates soft X-rays on the target. A 7 channel X-ray diode (XRD) is installed in the target chamber for the measurement of the total X-ray yield in the wide energy pass bands and the X-ray pulse shape. To measure the angular distribution of the X-ray yield, XRD can be attached to flanges located at every 15°, from 30° to 90° with respect to the target normal. To select an energy range, a filter can be

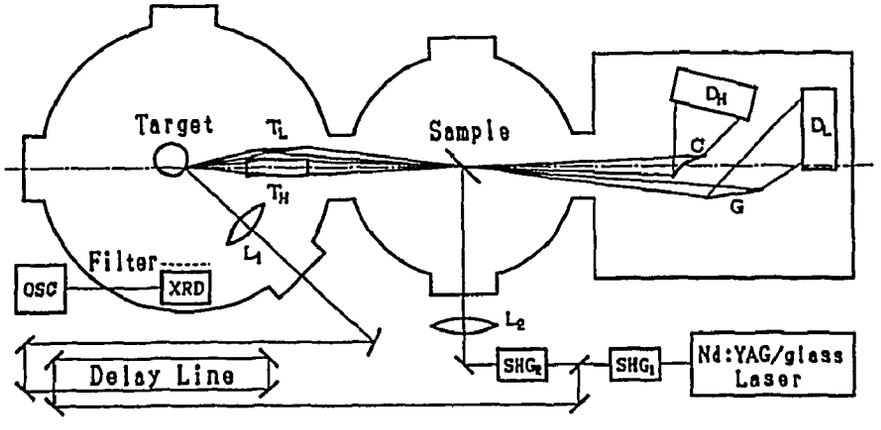

Fig.1(a): A schematic diagram of the spectrometer.

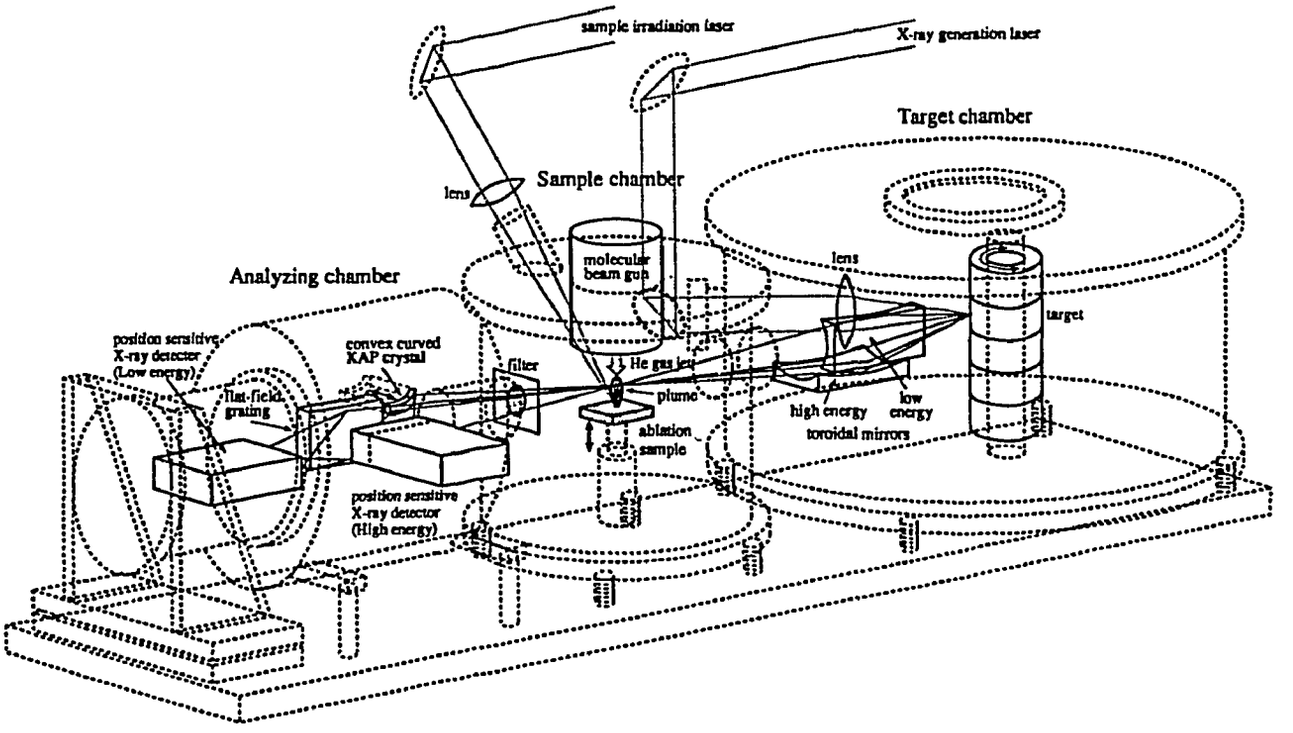

Fig.1(b): Schematic drawing of the time resolved X-ray absorption spectroscopy apparatus.

attached on each channel of XRD.

A part of the fundamental wave passes through the SHG_1, which is again frequency-doubled with SHG_2. A 1J, 532nm beam is generated and converged on the sample with a lens (L_2). A delay circuit (10~100ns) is installed in the 7J beam path to adjust the timing between sample irradiation and probing.

Figure 1(b) shows a schematic drawing of the spectrometer. Our spectrometer is designed to observe XAFS in rather wide energy range, 90eV to 3keV. However, it is difficult to analyze such a wide energy range by a simple polychromator. We have provided two sets of X-ray optical systems[7], one for lower energy region, from 90eV to 1000eV, and the other for higher energy region, from 1keV to 3keV. For both energy regions, toroidal mirrors (T_L,T_H) are used to collect and converge X-rays on the sample. X-rays are absorbed by the sample, and then arrive at the polychromator. In the lower energy region,

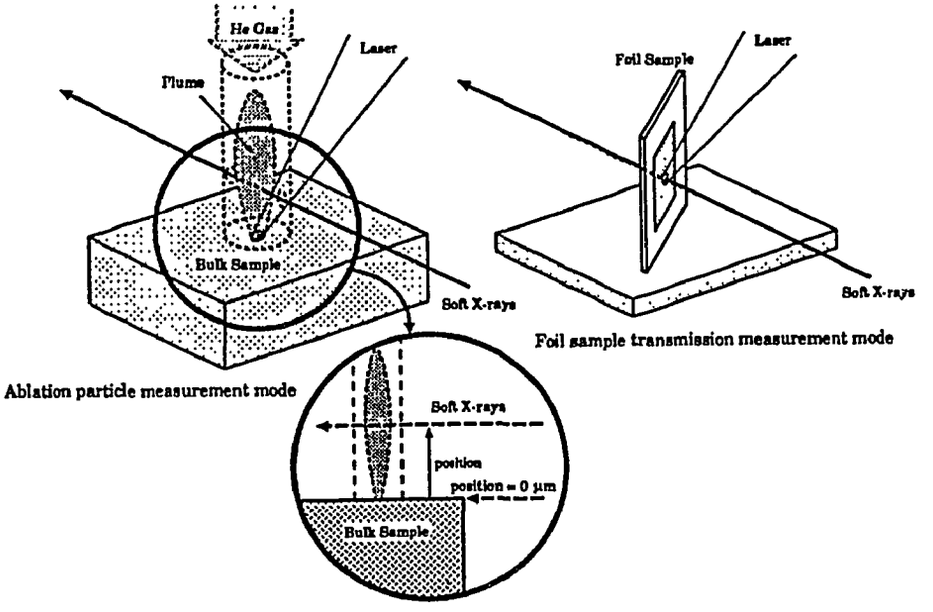

Fig.2: Schematic drawings of the sample measurement mode.

we use a grazing incident flat field grating (G) as an energy analyzer, and a 1024 channel MCP-PCD (D_L) as an X-ray detector. In the higher energy region, convex curved KAP crystal (C) and MCP-PCD (D_H) are used.

We have measured carbon near K-edge X-ray absorption spectra in two modes, the ablated particle measurement mode and the foil sample transmission measurement mode. Figure 2 shows schematic drawings of the sample measurement mode. In the ablated particle measurement mode, soft X-rays passes through the ablation plume which is generated by laser irradiation. The X-ray probing position is adjusted by sample surface. We have decided the probing position at which half X-rays are blocked by sample to be 0. We have also performed the X-ray absorption measurement in the helium gas environment. Helium gas jet has been synchronized with laser ablation to make a localized helium gas environment on the sample. An accumulation tube is attached on the sample to generate a localized helium environment effectively. In the foil sample measurement mode, irradiation laser is adjusted to the X-ray probe position to get dynamic behavior of the foil sample after laser irradiation.

3. RESULTS AND DISCUSSION

3.1. X-ray intensity

The total X-ray yields emitted from target materials were measured by X-ray diode (XRD). Table 1 shows the X-ray intensity and the conversion efficiency of the various target materials. Among then, gold has emitted the most intense X-rays. The total amount of emitted X-ray intensity reaches to 1.0×10^{16} photons/pulse and the conversion efficiency of the laser to X-rays is 4.6%. The number of photons incident on the sample is evaluated to be about 2×10^{11}photon/pulse. It is enough to get an absorption spectrum by only a single pulse of the laser produced plasma X-rays.

Table 1: The X-ray intensity and the conversion efficiency of the laser energy to soft X-rays.

	Total X-ray intensity [photons]	Conversion efficiency [%]	X-ray intensity on the sample [photons]
Au	1.0×10^{16}	4.6	1.8×10^{11}
Cu	8.2×10^{15}	3.7	1.5×10^{11}
Mo	7.6×10^{15}	3.4	1.3×10^{11}
Ti	5.3×10^{15}	2.4	9.5×10^{10}

3.2. Source X-ray spectra

Figure 3 shows the typical source X-ray spectra in the low energy region. The spectrum has been obtained by a single shot with a laser irradiance of 1×10^{13}W/cm^2. X-ray spectra of various targets differ from each other. In general, X-ray spectra of low-Z materials such as carbon (Fig.3(a)), contain many sharp line radiation peaks from multiply charged ion species, whereas those of high-Z materials, like gold (Fig.3(b)), exhibit rather continuum energy distributions. Thus, high-Z materials are suitable for the soft X-ray source of the absorption spectroscopy. In Fig.3(a) the X-ray source spectrum of carbon contains radiation peaks from

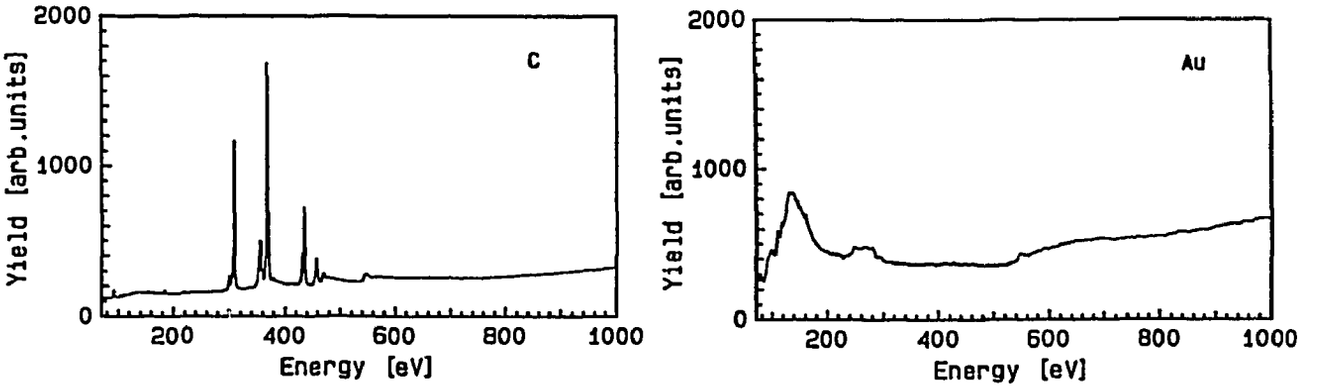

Fig.3: The source X-ray spectra from carbon and gold targets in the lower energy region.

1s→2p,3p,4p series transition of the C^{4+} and C^{5+}. In the part of 532nm irradiation laser measurements, gold has been used as an X-ray source. In the rest of measurements, hafnium target which generates more intense X-rays around the carbon K-absorption edge has been used.

For the energy calibration and the determination of the energy resolution of the spectrometer, an observed spectrum was compared with a simulated spectrum[8]. Thus, energy resolutions of our spectrometer were found to be 0.8eV, 2.0eV, 10eV and 8eV in energy ranges of 100~200eV, 200~500eV, 500~1000eV, 1~3keV, respectively.

3.3. X-ray absorption spectra of graphite

As a reference of the absorption edge and peaks of the large carbon cluster, X-ray absorption spectrum of carbon foil was measured(Fig.4). The spectrum consists of an absorption peak at around 285eV followed by broad absorption, the maximum of which lies around 295eV. The absorption peak at around 285eV corresponds to carbon 1s→π* transitions in molecules containing π electrons. The carbon foils have many π electrons due to sp^2 hybridization and hence the peak intensity at 285eV is high. The broad maximum between 290eV and 310eV is assigned to 1s→σ* band transitions.

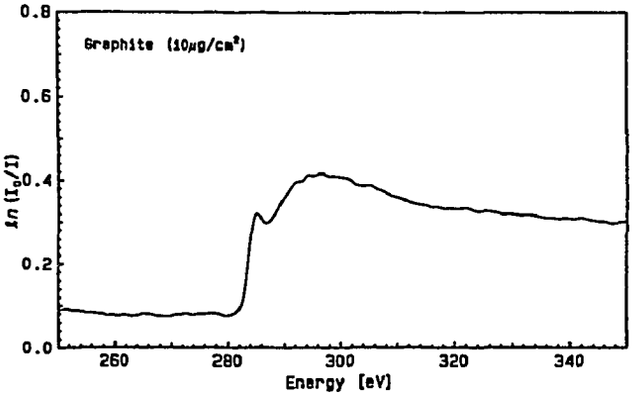

Fig.4: The X-ray absorption spectrum of the graphite (10μm/cm^2).

3.4. The properties of ablation process of carbon

Figure 5 shows spatial dependence of the ablated carbon species. The energy density of the irradiation laser on the sample is about 20J/cm^2 and the delay times between laser irradiation and X-ray probing are 40ns and 120ns. The spectra exhibit a main absorption edge and peaks.

The absorption edge at 296.5eV is from 1s→vacuum level transition, and the absorption peaks, 284.3eV, 288eV and 293eV are originated from 1s→2p transition of neutral carbon atom(C^0), C^+ and C^{2+} ions, respectively[9]. The absorption peak, 281eV is also observed. This peak energy is lower than C^0, thus it is considered to be a peak originated from negative charged ions(C^-).

Figure 6 shows the spatial distribution of the ablated carbon particles. We have not made any corrections for the shape of the ablation plume or the absorption cross section. The absorption peak originated from neutral carbon is stronger as the probing position is closer to the sample surface and remains strong near the surface even when X-ray probing delay time extends to 120ns. On the contrary, C^{2+} peak is observed more than 2mm from the surface when delay time is 120ns. Therefore, at the initial stage, the speed of C^{2+} ion is more than 1.5×10^6cm/s. The absorption peak of the neutral carbon decreases in inverse proportion to the distance from the surface. On the other hand, the absorption peak of C^- decreases rapidly and the peak of C^+ decreases gradually more than that of the neutral carbon. This situation suggests: 1) Lowly ionized and neutral carbons are emitted from the sample surface even

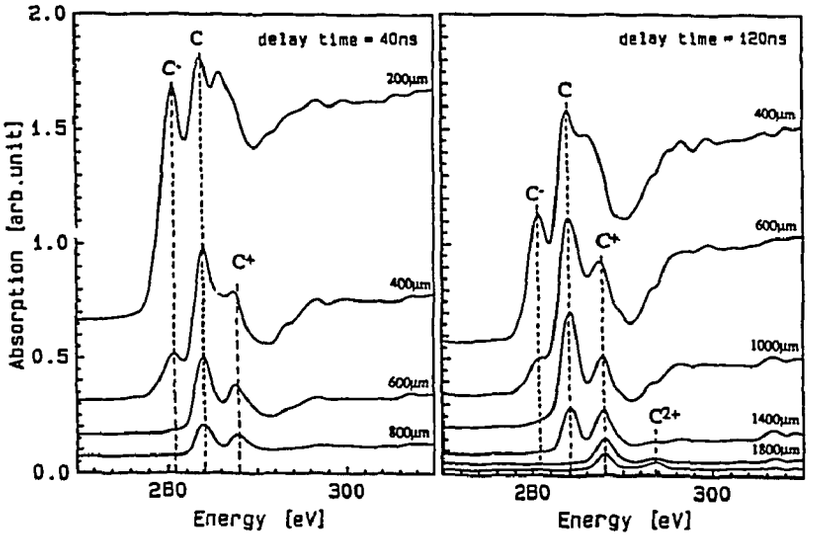

Fig.5: Spatial dependencies of the ablated carbon species.(laser energy density: 20J/cm^2)

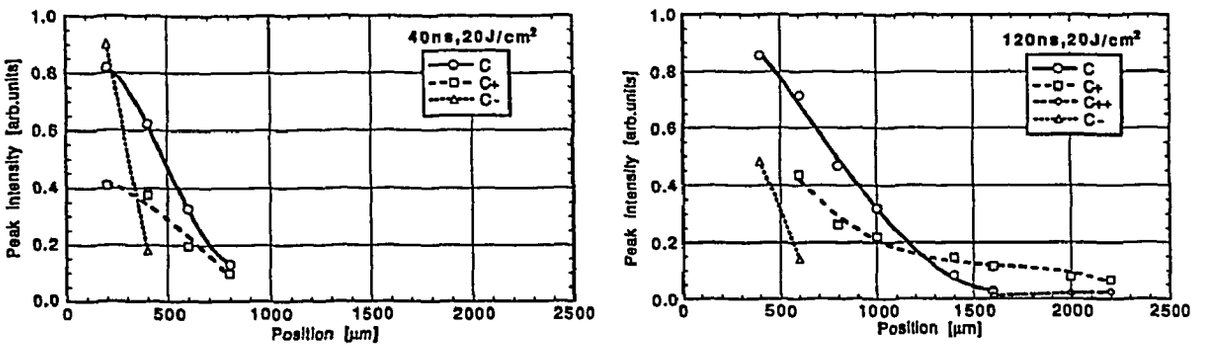

Fig.6: Spatial distribution of the ablated carbon species.(laser energy density: 20J/cm^2)

after laser irradiation. 2) Two distinct effects exist in the acceleration of the particles. One is the Coulomb repulsion effect by the transient electric field. This effect accelerates charged particles in proportion to the ionization level. The other is a hydrodynamic expansion from the sample surface to vacuum. This effect continues even after the laser irradiation, and accelerates neutral atoms and ions equivalently.

3.5. Ablated carbon particles in the helium gas environment

In the rare gas environment, it is expected that ablated particles are cooled by collision with rare gas atoms and clustering is promoted. Helium gas jet is synchronized with laser ablation to make a localized helium gas environment on the sample. Figure 7 shows the X-ray absorption spectra with and without helium gas. In the region close to the sample surface, the neutral carbon (C^0) peak in the helium gas environment is equivalent to that in vacuum. However, at the top of the ablation plume, the C^0 peak height reduces with helium. The C^+ peak in the helium gas environment remains almost equivalent to the peak in vacuum. Even

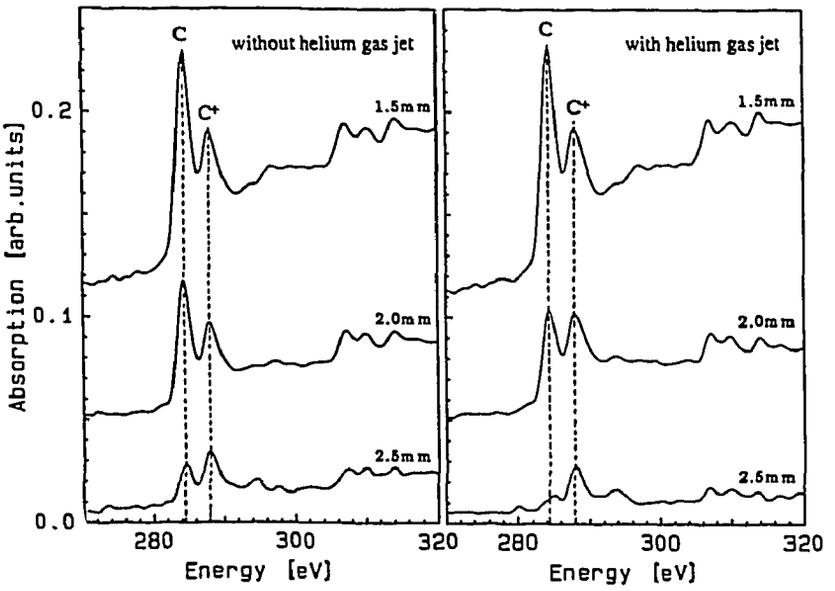

Fig.7: The depression effect of the helium gas environment. X-ray absorption spectra of the laser ablated carbon. (laser energy density: 5J/cm^2, delay time: 120ns.)

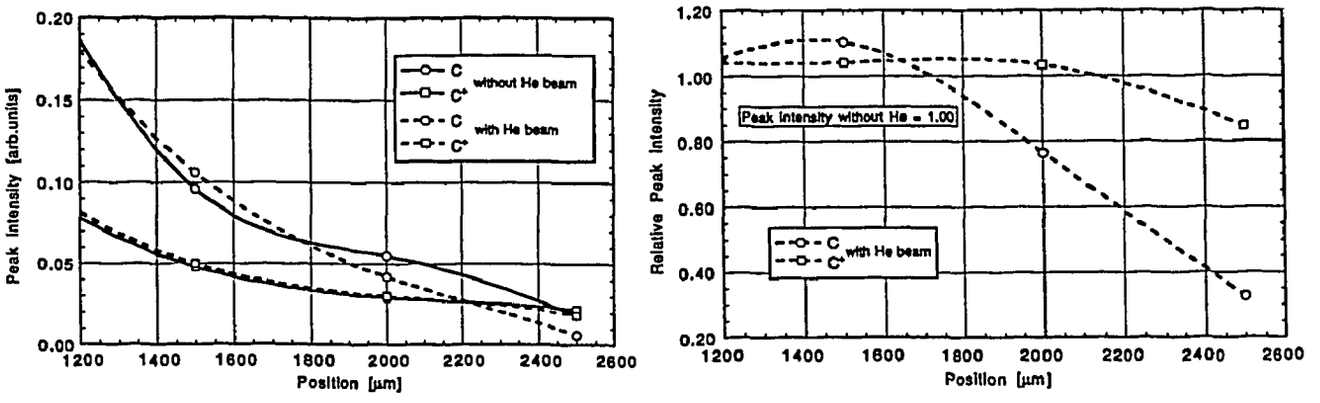

Fig.8: The depression effect of the helium gas environment. Spatial distribution of the ablated carbon species. (laser energy density: 5J/cm^2, delay time: 120ns).

at the top of ablation plume, there are no additional absorption peaks originated from small carbon clusters, such as C_2 or C_3. These results suggest following possibilities. In the helium gas environment, the expansion of the ablation plume brings about compression of the helium gas, and makes a dense helium region at the top of ablation plume. The dense helium cloud depresses the free expansion of the ablation plume. Thus, what can be seen at 2.5mm above the sample surface in vacuum appears at about 2.2mm in the helium environment. The helium cloud effect has been observed at longer delay time experiments before[10]. We have observed a depression effect even when the delay time is 40ns.

4. CONCLUSIONS

The time evolution of the electronic structures of laser ablated carbon particles and their spatial distributions were measured by the X-ray absorption spectroscopy using LPX as an X-ray source. In the energy range of carbon K-edge, the absorption peak originated from 1s→2p transition of neutral carbon atom and both positive and negative ions were observed. Lowly ionized and neutral carbons were emitted from the sample surface even after laser ablation. The ablated particles were accelerated by the Coulomb repulsion effect and hydrodynamic expansion. In the helium gas environment, dense helium cloud was generated on the top of ablation plume. The helium cloud depressed the free expansion of the ablation plume. Up to 120ns delay time range, no absorption peaks assigned to small clusters were observed.

REFERENCES

1) H.C.Gerritsen, H. van Brug, F.Bijkerk and M.J. van der Wiel, J.Appl.Phys. 59, 2337 (1986).
2) D.J.Nagel, Adv.X-ray Anal. 1, 1 (1975).
3) K.Murakami, H.C.Gerritsen, H. van Brug, F.Bijkerk, F.W.Saris and M.J. van der Wiel, Phys.Rev.Lett. 56, 655 (1986).
4) H.W.Kroto, J.R.Heath, S.C.O'Brien, R.F.Curl and R.E.Smalley, Nature 314, 162 (1985).
5) H.S.Carman,Jr. and R.N.Compton, Proc.2nd Inter.Conf. Laser Ablation, (1993).
6) A.Gupta, B.W.Hussey, A.Kussmaul and A.Segmuller, Appl.Phys.Lett. 57, 2365 (1990).
7) A.Miyashita and O.Yoda, JAERI-M Report 88-212 (1988).
8) A.Miyashita, O.Yoda, K.Murakami, T.Ohyanagi, S.Aoki and N.Yamaguchi, Proc.Laser Advanced Materials Processing '92, 1029 (1992).
9) E.Jannitti, P.Nicolosi and G.Tondello, Physica Scripta 41, 458 (1990).
10) D.B.Geohegan, Appl.Phys.Lett. 60, 2732 (1992).